

# Using QCLs for Studying Exceptional Point Singularities



November, 2022  
Page 1

## ABSTRACT

Researchers from Switzerland have developed a more practical and robust method for studying the effects of exceptional point (EP) singularities. As lasers provide an ideal system for direct observation and engineering of spectral singularities, two dual section distributed feedback (DFB) quantum cascade lasers (QCLs) were designed with Fabry-Perot modes and quarter wave shifted (QWS) DFB modes. By varying the physical location of the QWS defect as well as the injection current, researchers were able to observe and study EPs based on the coupling parameters of the system. These results show that the developed QCL is a perfect platform to study and further the knowledge of EPs and the effects they have between the weak and strong coupled regime of a laser.

## EXCEPTIONAL POINTS

Exceptional points (EPs) can have dramatic effects on many physical properties in the world today. Although these singularities only appeared as solely mathematical outcomes in previous decades, the physical materialization of EPs has been previously demonstrated in laboratories in non-Hermitian systems. A non-Hermitian system is a local system that does not conserve energy, or one with gains and losses. The captivating aspects of these types of systems are focused around EPs.

An exceptional point is when two or more eigenvalues and the corresponding eigenvectors coalesce and become degenerate.<sup>1</sup> An  $n \times n$  matrix can have  $n$  eigenvalues, but this doesn't necessarily mean that there are  $n$  distinct eigenvalues. In the case where multiple eigenvalues are identical, they are identified as degenerate. In a system that has a certain level of variability, the mathematical model representing this system, with a corresponding matrix, will also change. When two or more of the eigenvalues in the model matrix become identical or degenerate because of the changing nature of the system, they coalesce. At this time, an EP has occurred and can be further studied.

Lasers have become interesting systems by which researchers can look closer at EPs. Because lasers exhibit gains and losses, they are considered non-Hermitian systems - a more recent area of study with promising results. With gain and loss introduced in lasers, the occurrences of EPs can dramatically affect the overall response of the system. EPs also mark the boundary between the weakly and strongly coupled regime, adding to the usefulness of EP research.<sup>1</sup> Other effects can be introduced because of EPs connected to the two-fold degeneracy (in real and imaginary part) of the eigenvalues in multi-section distributed feedback (DFB) lasers.

## EIGENVALUES & EIGENVECTORS

A matrix is often used to represent a mathematical object or system. Matrix **A**, below, is an array with  $m$  number of rows and  $n$  number of columns. The entries in matrix **A** are symbolized with  $a_{i,j}$ , where  $i$  and  $j$  indicate row and column numbers with the maximum being  $m$  and  $n$ , respectively.

$$A = \begin{bmatrix} a_{11} & a_{12} & \cdots & a_{1n} \\ a_{21} & a_{22} & \cdots & a_{2n} \\ \vdots & \vdots & \ddots & \vdots \\ a_{m1} & a_{m2} & \cdots & a_{mn} \end{bmatrix}$$

An eigenvector  $\vec{v}$  is, by convention, an  $m \times 1$  matrix. An eigenvector is a vector that, when linearly transformed, does not change direction. The eigenvector  $\vec{v}$  of a given matrix **A** is the vector for which the following eigenvector equation holds true:

$$A \vec{v} = \lambda \vec{v}$$

where  $\lambda$  is a scalar value, called an eigenvalue corresponding to that eigenvector. The transformation **A** on vector  $\vec{v}$  is completely defined by the eigenvalue,  $\lambda$ . There are many special properties associated with eigenvectors and eigenvalues diving deeper into the field of mathematics.

The effects of EPs can naturally be seen in many applications in physical problems: mechanics, electromagnetism, atomic and molecular physics, quantum phase transitions, quantum chaos, and much more.<sup>2</sup> In the last few years, researchers have been focusing on and making significant progress in the field of optics, both in the theoretical realm as well as in experimental applications. Optics, as of now, is one of the most practical venues of exploration to further the understanding of exceptional point physics. EPs promise to advance highly sensitive sensor applications, but as an emerging field, much still needs to be discovered about these optical phenomena. The study of EPs will provide behavioral details and advance theoretical understanding.

## PROBLEMS AND GOALS

To study exceptional points, a few systems can be constructed. Previously, researchers have explored coupled photonic crystal nanolasers with asymmetric optical gains

and losses leading to phase transition of lasing modes at the EP singularity. Others have investigated coupled micrometer-sided cavities, also with asymmetric gain and loss, that feature controlling intercavity coupling strength.<sup>1</sup> While these methods do work for expanding the understanding of EPs and the features they introduce to the vicinity around them, they can still prove to be quite challenging and precise, and a calculated setup is needed. A more simple and practical approach is needed to access these physical EPs to investigate the phase transitions around them.<sup>1</sup>

As previously discussed, lasers can be a practical method for studying these spectral singularities. Within coupled laser cavities, EPs can lead to either pump-induced or loss-induced revival of lasing. This is where the gain and loss come into play surrounding the EP singularity. Phase transition and self-pulsation effects can be further researched by using lasers, specifically multi-section distributed feedback (DFB) lasers.<sup>1</sup>

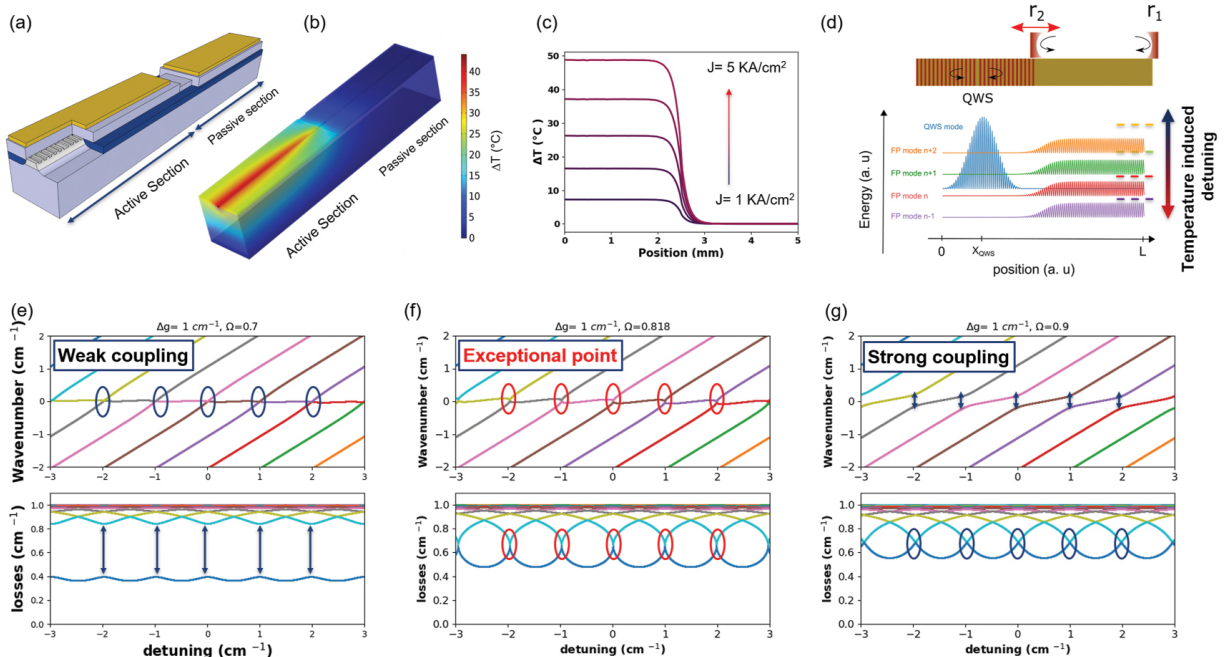


**Figure 1.** The concept of the coupling in dual section DFB QCLs. (a) Schematic of a dual section DFB QCL with quarter wave shift (QWS) defect in each section. The electrically driven section is labeled as active section. (b) Finite element simulation of the thermal distribution along the laser performed by COMSOL Multiphysics, when driving one section of device. The color code in the 3D view of device represents the temperature difference to the substrate. (c) The line cut of the temperature difference along the laser ridge for different injection current densities in the laser. (d) Top: the schematic showing the two cavities: the DFB grating cavity with a QWS defect on left side and the FP cavity made by the laser facet reflector ( $r_1$ ) and reflection from the DFB grating ( $r_2$ ) on the other side. Bottom: the schematic of the field intensity for the QWS mode and the closest FP modes to that, that fall in the stop-band of the grating spectrum. The intensity plots are shifted vertically to show their energy difference. (e)–(g) Illustration of the real part (frequency) and the imaginary part (losses) of the eigenmodes of the Hamiltonian, consisting of a single DFB mode coupled to multiple FP modes. From left to right, depending on the value of  $\Omega/\Delta g'$ , system undergoes weak coupling regime (mode repulsion in imaginary part), exceptional point (coalescence of the modes in both real and imaginary part), and strong coupling regime (repulsion of the modes in real part of eigenvalues, similar to strong coupling in Hermitian systems).<sup>1</sup>

## METHOD

Researchers from the Institute for Quantum Electronics, ETH Zürich, Switzerland have developed two dual section DFB quantum cascade lasers (QCLs) with the ability to operate at different coupling regimes. The concept of the coupling in the dual section DFB QCLs can be seen in **Figure 1**. In both of these QCLs, different coupling regimes are demonstrated through the Fabry-Perot (FP) modes and the quarter wave shift (QWS) DFB mode allowing interpretation through a non-Hermitian dynamics model for EP exploration.<sup>1</sup> The two sections of the laser are designed to emit at different wavelengths: 4.3  $\mu\text{m}$  and 4.6  $\mu\text{m}$ . There is also an etched top layer that allows for electrical isolation, so each section can be independently driven or pumped. Only one section is pumped at a time, making one section "active" and the other "passive." Each device has slightly different positions for the QWS defect from the FP cavity.

The design parameters, such as the physical distance of the QWS defect from the FP cavity, and the electrical parameters, such as the injection current, can be adjusted to change the coupling strength in the designed DFB QCLs. Different injection current densities determine the temperature difference along the laser ridge line as seen in **Figure 1c**.

The eigenmodes are a key piece in **Figure 1e-g** as the coupling changes from the weak regime to the exceptional point and finally to the strong regime. The critical portion of the illustration of the EP is where the real and imaginary part of the eigenmodes of the Hamiltonian coalesce. This marks the boundary between the weak and strong coupled regime.

Here, researchers operate the two devices at different regime of coupling to show the effects of the EPs. The results are shown in the next section to exhibit how the laser dynamics can be strongly modified by the strength of the interaction of modes and the existence of the EP degeneracy.<sup>1</sup>

## RESULTS

The two devices, a 4 mm QCL and a 5 mm QCL, had slightly different physical parameters. Device 1 (**Figure 2**) utilized the QWS defect location in the middle of the front and back sections, while Device 2 (**Figure 3 & Figure 4**) utilized the QWS defect location shifted closer to the facets, offset from the middle, as well as slight changes in the grating refractive contrast. This physical change, as well as with varying injection current, determine how the complex eigenvalues move closer to the EP.

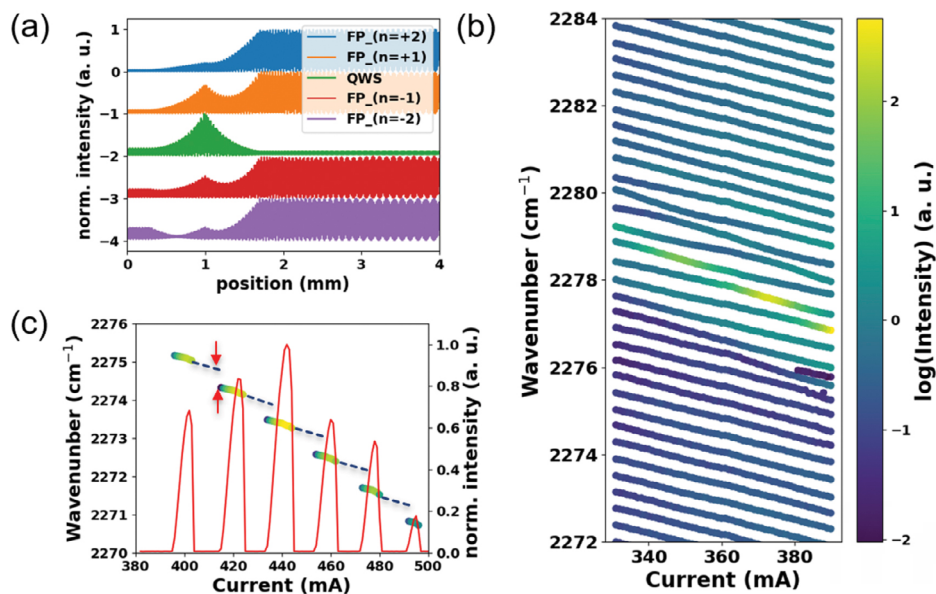


**Figure 2. Strong coupling of FP modes to the QWS DFB modes. (a)** The intensity profile of the QWS mode and its closest FP modes extracted from TMM simulations for a 4 mm long dual section DFB QCL (device 1), where the QWS on is positioned at the middle of the driven section and the grating refractive contrast was estimated to be  $\Delta n/n \approx 0.5\%$  from the width of the DFB stop-band. The position of the QWS defect in the grating and length of the device allows relatively large overlap of the mode profiles. **(b)** The measured sub-threshold spectral map of the device. The QWS mode is distinguished by the highest intensity mode in the middle of photonic gap, and anti-crosses with FP modes. **(c)** Spectral map of the device at driving currents above threshold. The QWS lasing mode turn on and off multiple times, and there is a clear energy gap between each turning off point (marked by dashed lines) and the consequent turning on point. The integrated optical intensity of the QWS mode is plotted in red.<sup>1</sup>

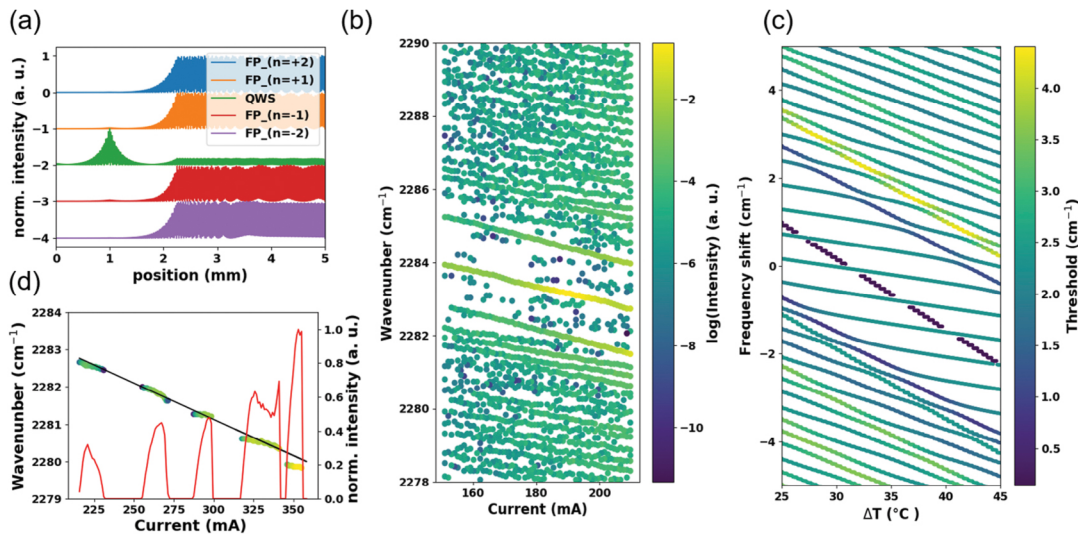


**Figure 3.** Multiple occurrence of EP over the dynamic range of DFB QCL. (a) The intensity profile of the QWS mode and the closest FP modes to that as function of position along the device extracted from TMM simulations, for a 5 mm long dual section DFB QCL (device 2), where the QWS is positioned at  $0.4 \times L_B$ . The grating refractive index contrast was estimated to be  $\Delta n/n \approx 0.6\%$  from the width of the DFB stop-band. (b) Measured spectral map of the device at sub-threshold currents. The map is obtained when driving the DFB section corresponding to the observation frequency. The absence of the mode repulsion and still strong modulation of the intensity of the QWS mode are the remarkable differences compared to strong/weak coupling regime. (c) TMM simulation results for the grating structure of the device, including the temperature profile along the device waveguide as function of the injected current. The QWS mode crosses in both real (frequency) and imaginary part (losses) when the FP modes tuned to be in resonance with the QWS DFB mode. (d) The measured spectral map of the device when driven above threshold. One distinct feature here is the absence of the frequency gaps between the subsequent off/on points, consistent with the absence of anti-crossing in the sub-threshold spectral map. The integrated intensity of the QWS mode is shown by the red solid curve, distinguishes the dynamics in this case from weak coupling regime.<sup>1</sup>

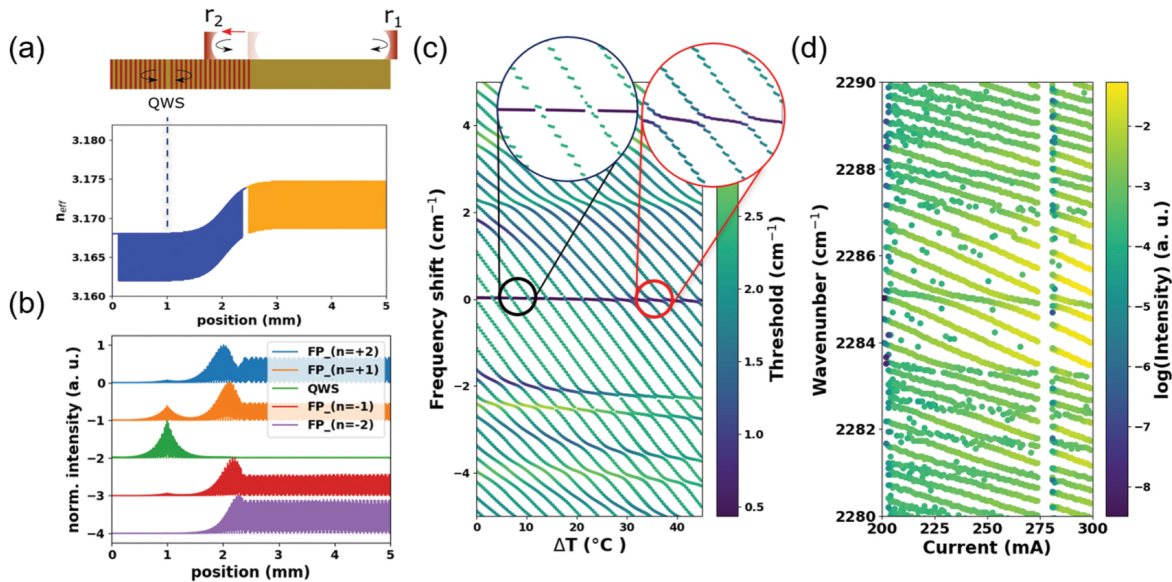
Figure 2 shows the intensity profile from simulation, the measured sub-threshold spectral map, as well as the measured above threshold spectral map for the 4 mm long QCL with the QWS defect in the middle of the front and back section. The intensity profile shows a relatively good overlap of the QWS DFB mode and its closest FP modes. This overlap is critical for determining the exact location of the EP singularities. The sub-threshold spectral map shows anti-crossing between the frequency of the main QWS mode and detuned FP modes. This is what we expect when the QCL is driven with current below the lasing threshold. At above threshold current, however, there are obvious signs of strong coupling dynamics. Overall, when current is pumped above threshold, the laser switches on and off multiple times (Figure 2c) while emitting a single mode output. A frequency jump is seen at each turn off and on location, relating to the observed anti-crossing gap in the sub-threshold experiment.<sup>1</sup>

Figure 3 shows the same three profiles and maps, and it also includes simulation results for the grating structure of the 5 mm long QCL with the QWS defect shifted toward the facets. Here we see the overlap of the modes to be much lower (Figure 3a). There is also an absence of anti-crossing between the modes when driven with current below the threshold, compared to Device 1. The grating refractive index contrast is also slightly altered from  $\Delta n/n \approx 0.5\%$  to

$\Delta n/n \approx 0.6\%$ . This physical difference can also affect EPs. Figure 3c suggests the two-fold degeneracy (real and imaginary part) of the DFB mode with FP modes at crossing points.<sup>1</sup> Once again we see the device switching on and off again, but this time without the energy gaps.

Device 2 (offset QWS defect) shows that other methods, such as device design parameters, can determine the movement of the complex eigenvalues close to the EP singularity. Previously, external disruption elements or asymmetrical pumping were the only experimentally proven methods. Now, physical design parameters, such as length of the device, QWS defect location, or the refractive index contrast of the DFB grating can alter the occurrences of EPs in experiments. These dual section devices provide more degrees of freedom when tuning of the coupling strengths is required.<sup>1</sup>

Figure 4 swaps the pumped section and passive section. This results in the EP degeneracy being lifted and the system moves toward strong coupling. This means that the system has moved from a weak coupled state to a state with an EP singularity. Then the system moves toward the strong coupled state, eliminating the EP degeneracy. Figure 4c shows the system moving from the EP regime to the strong coupling regime due to temperature changes from different electrical pumping schemes. Because the EP singularity marks the boundary between the weak and



**Figure 4.** Lifting the EP degeneracy by different electrical pumping schemes. (a) The effective refractive index profile along the waveguide of laser, where the QWS defect location is marked by dashed line at  $x = 0.4 \times L_B$ . The device is driven electrically in the counterpart section (the orange color) of the one with DFB designed at the observation wavelength. The inset shows schematically the impact of the temperature profile induced by changing the electrically pumped section, as a shift of the reflection point for the FP modes inside the DFB grating ( $r_2$ ). (b) Intensity profile of the QWS mode and the four closest FP neighbor modes as function of position along the laser waveguide, extracted for  $\Delta T = 35^\circ\text{C}$  from TMM simulations. As a result of the extension of the heating profile toward the target DFB section, the intensity profile of FP modes penetrates more in the DFB section. (c) The simulated spectral map at sub-threshold current densities. As a consequence of the increased overlap between the FP modes and the QWS mode intensity, the coupling strength  $\Omega$  is increased by increasing the temperature difference between the two section  $\Delta T$ , and the FP modes starts to repel the QWS modes. The insets highlight the onset of coalesce of modes and anti-crossing of modes in real parts for different values of  $\Delta T$ . (d) The measured sub-threshold spectral map of the device, where EP degeneracy is clearly lifted at the applied current range to the device.<sup>1</sup>

strongly coupled regimes, **Figure 4** suggests that this method can hit the exact EP degeneracy condition between the coupling regimes.

These dual section DFB QCLs provide a practical and robust method for studying the effects of exceptional point (EP) singularities. This non-Hermitian system modified physical design parameters, rather than just varying electrical and optical pumping, to show the effects of the EP degeneracy on the laser dynamics. The simplicity of these DFB QCLs provide a new and promising design for exploring exceptional point singularities and the effects they can have on their surroundings.

## WAVELENGTH'S ROLE

Due to the temperature dependence on the injection current of the QCL, researchers upgraded the electronic drive equipment to utilize the high performance capabilities of Wavelength Electronics' QCL driver. This critical component enables the sensitive measurements and analysis of EP degeneracy in QCLs and other non-Hermitian systems.

Because the EP degeneracy is lifted at only a certain applied current, ultra-low noise laser drivers were needed. Wavelength Electronics' QCL2000 OEM driver limits noise produced to as low as 1.3  $\mu\text{A}$  RMS up to 100 kHz and an average current noise density of 4  $\text{nA}/\sqrt{\text{Hz}}$ . With an output of up to 2 A and stability around 10 ppm long-term, the QCL2000 provided the stability and flexibility needed for EP research. Additional features include: current limit and setpoint, remote capabilities, and bandwidth of 2-3 MHz.

The stability of the injected current into the DFB QCL, allowed researchers to discover the precise applied current at which the EP degeneracy was lifted. This project, aided by the QCL2000 OEM, suggests a more practical and flexible design for exploring the effects of EPs in non-Hermitian photonic coupled systems.

## REFERENCES

1. Shahmohammadi, M., Suess, M. J., et. al.: Exceptional point singularities in multi-section DFB lasers, *New J. Phys.* **24** 053047 (2022). <https://doi.org/10.1088/1367-2630/ac6d6f>
2. Heiss, W. D.: The physics of exceptional points, *Journal of Physics A: Mathematical and Theoretical* **45** 444016 (2012). <https://doi.org/10.1088/1751-8113/45/44/444016>

## USEFUL LINKS

- QCL2000 OEM [Product Page](#)

## PERMISSIONS

Figures 1, 2, 3, & 4 in this case study were obtained from Reference 1. The article (Ref. 1) is distributed under terms of Creative Commons Attribution 4.0 International License (<https://creativecommons.org/licenses/by/4.0/>), which permits unrestricted use, distribution, and reproduction in any medium, provided that you give appropriate credit to the original authors and the source, provide a link to the Creative Commons license, and indicate if changes were made.

No changes were made to the images. They are presented here in their original form. The caption for Figure 1 was edited for length. No other changes were made to the other captions.

### PRODUCTS USED

QCL2000 OEM

### KEYWORDS

Exceptional point, EP, singularity, distributed feedback, DFB, laser, quantum cascade laser, QCL, degeneracy, dual section, eigenvalue, eigenvector, matrix, laser driver

### REVISION HISTORY

Document Number: CS-LD06

REVISION	DATE	NOTES
A	November 2022	Initial Release